Anomalous sound attenuation in liquid $Te_{50}Se_{50}$ mixture under high pressure

2000 J. Phys.: Condens. Matter 12 7323

(http://iopscience.iop.org/0953-8984/12/33/302)

J. Phys.: Condens. Matter **12** (2000) 7323–7339. Printed in the UK PII: S0953-8984(00)13921-9

Anomalous sound attenuation in liquid $Te_{50}Se_{50}$ mixture under high pressure

M Yao, N Itokawa, H Kohno†, Y Kajihara and Y Hiejima

Department of Physics, Graduate School of Science, Kyoto University, Sakyo-ku 606-8502, Kyoto, Japan

E-mail: yao@scphys.kyoto-u.ac.jp

Received

Abstract. The sound velocity, v, and the sound attenuation coefficient, α, have been measured for liquid $Te_{50}Se_{50}$ mixture at 20, 32 and 43 MHz in the temperature and pressure range up to 1000 °C and 150 MPa. Near the melting point α decreases with increasing temperature, as is expected from the temperature variation of shear viscosity. In addition to the normal behaviour, we have found two peaks of α in the temperature range where the semiconductor-to-metal transition is observed. One is the high temperature peak, which appears around 850 °C irrespective of the frequency, and the other is the low temperature peak, whose position depends strongly on the frequency. The peaks become more prominent with increasing pressure, indicating the importance of the inter-chain couplings. Assuming a Debye-type relaxation for the frequency-dependent adiabatic compressibility, we have estimated the relaxation time to be about 7 ns from the high temperature peak.

1. Introduction

Recently we have measured the sound attenuation coefficient, α, of expanded liquid mercury, and in addition to the critical attenuation we have observed the secondary maximum in the density dependence of α at a density near 9 g cm^{-3}, where the metal–nonmetal (M–NM) transition occurs [1, 2]‡. Assuming a Debye-type relaxation for the frequency-dependent adiabatic compressibility, we have estimated the relaxation time to be of the order of nanoseconds, and suggested that slow dynamics is generated by the sound pressure in the M–NM transition range [1, 2]. This new finding arouses an interesting question of whether such slow dynamics could be observed in other liquid systems that undergo the M–NM transition. In the present work we study the acoustic properties of liquid $Te_{50}Se_{50}$ mixture, which is transformed from a semiconductor to a metal at a moderate temperature by heating up [4].

Although both selenium and tellurium are well known crystalline semiconductors, Te is changed to a liquid metal on melting unlike Se. Near the melting point liquid Se consists of twofold coordinated polymeric chains with bond angle similar to that of the crystalline helical chain and broad distribution of the dihedral angle [5]. The chain length becomes shorter with increasing temperature [6] and near the critical point it is estimated to be about seven atoms [7]. There have been frequent disputes about the structure of liquid Te since early experimental [8] and theoretical [9] investigations. Recently it has been suggested that liquid

† JSPS Research Fellow.

‡ A similar observation was reported subsequently by Kozhevnikov *et al* [3].

0953-8984/00/337323+17$30.00

Te is also composed of chain fragments [10], which are formed by the normal covalent bonds and the elongated covalent bonds due to the inter-chain interactions [11–13].

In liquid Te–Se mixtures the semiconductor-to-metal (S–M) transition occurs in relatively narrow temperature range, which moves to higher temperatures with increasing Se concentration [4, 14]. The S–M transition is accompanied by a structural change from an Se-like loosely packed structure to a Te-like densely packed structure [15–17], and it was recognized as an example where the liquid–liquid phase transition is blurred due to fluctuations [18]. Near the transition temperature thermodynamic anomalies such as the minimum of the sound velocity [18–20] and the maximum of the specific heats [21–23] were observed.

All the studies mentioned above were mainly aimed at investigating the static properties of liquid chalcogens. However, since the most characteristic feature of the liquid state, compared with the solid state, is the time evolution of the atomic arrangement, it would be very interesting to study dynamic aspects of the S–M transition. As to the liquid Te–Se mixtures, the measurements of the viscosity [24] and thermal conductivity [25] are a few examples that are concerned with dynamic properties, though both quantities exhibit no anomalous behaviours even in the S–M transition range.

In the present study we have found anomalous sound attenuation in liquid $Te_{50}Se_{50}$ mixture. The remainder of this paper is divided as follows. We will describe the experimental method for the acoustic measurements in section 2 and the experimental results in section 3. The results show a strong and complicated dependence on temperature, pressure and frequency. Analysing the data in section 4, we will show that there appear two peaks in the temperature variation of α. In section 5 we will estimate the relaxation times and discuss a possible mechanism for the relaxation. Finally a brief summary will be given in section 6.

2. Experimental procedure

The sound velocity, v, and the sound attenuation coefficient, α, have been measured for liquid $Te_{50}Se_{50}$ mixture at 20, 32 and 43 MHz in the temperature and pressure range up to 1000 °C and 150 MPa. The mixture was prepared from 99.999% purity Te and Se. The experiments were carried out at nearly constant pressures. Figure 1 shows the state-points where the ultrasonic measurements have been made.

The experimental apparatus for the ultrasonic measurements is shown in figure 2. Quartz rods 8 mm in diameter were used as buffer rods for transmitting the ultrasonic waves. Two quartz rods, A and B, were inserted into a quartz tube with the inner diameter of 8 mm and the outer diameter of 10 mm. The axial length of both quartz rods was 95mm. A gap between the two rods served as the sample part and the sample length l_S was 7.4 mm for the measurements at 20 MHz, 6.0 mm at 35 MHz and 1.8 mm at 43 MHz. Similar ultrasonic cells made of sapphire [1] or sintered alumina [19] were described in detail.

The temperature of the sample part was raised by a heater surrounding the central part of the cell, and monitored by chromel–alumel thermocouples. The temperature was calibrated by detecting the melting of zinc ingots put in the sample part. The cell assembly was set in a steel high-pressure vessel which was pressurized with argon gas. The pressure was measured by a Heise gauge. The experimental errors in temperature and pressure were ± 8 °C and ± 0.5 MPa, respectively.

The sound velocity, v, was measured by an ultrasonic pulse transmission/echo method [26]. Z-cut $Pb(Zr \cdot Ti)O_3$ transducers were bonded to the cold ends of quartz rods. For 20 MHz we used the fundamental resonance frequency, and for 32 and 43 MHz we used the third harmonics. The time required for an ultrasonic pulse to traverse from one transducer to the other, τ_{AB}, and the time required for an echo to return from the interface between the rod A (or

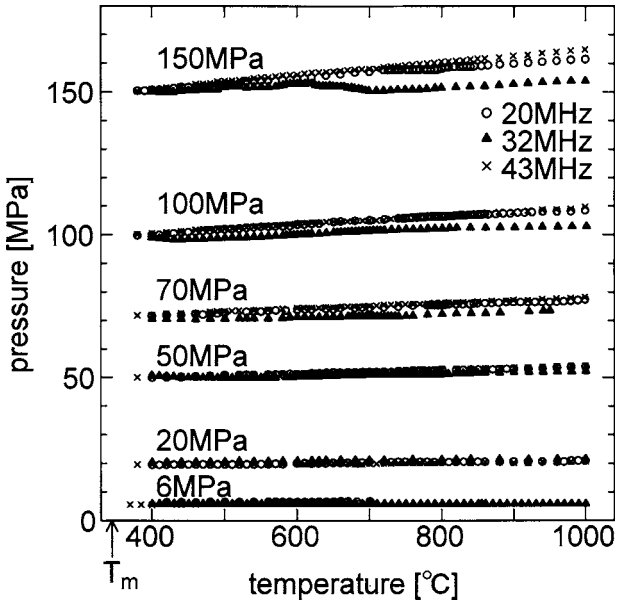

Figure 1. The state-points of the present ultrasonic measurements are plotted on the P–T plane. Three different symbols are used depending on the frequency. The melting point, T_m, of $Se_{50}Te_{50}$ (345 °C) is indicated by the arrow.

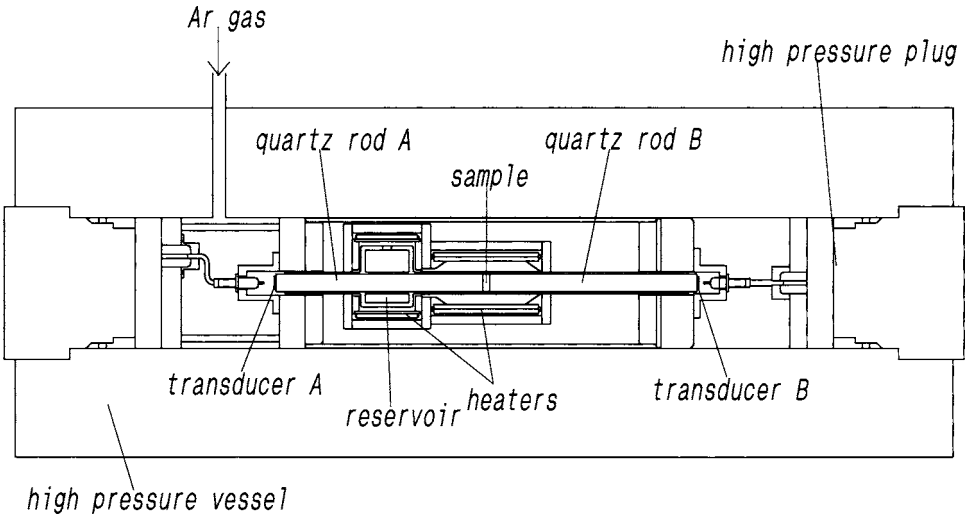

Figure 2. The experimental apparatus for measuring the sound velocity and attenuation for liquid $Te_{50}Se_{50}$ under high temperature and pressure.

B) and the sample, τ_{AA} (or τ_{BB}), were measured. All the signals were accumulated 100 times and recorded with a digital oscilloscope. The difference between τ_{AB} and $(\tau_{AA}+\tau_{BB})/2$ gives the time required for the pulse to traverse the sample. Then v can be deduced from

$$v = l_S/\{\tau_{AB} - (\tau_{AA}+\tau_{BB})/2\}. \tag{1}$$

The error in v was less than 2% at 20 MHz, 3% at 32 MHz and 5% at 43 MHz.

The sound attenuation coefficient α can be deduced from

$$\alpha = -\ln T_S / l_S \tag{2}$$

where T_S is the transmission rate through the sample. Since it is difficult to change l_S *in situ* under high temperature and pressure, we have adopted an alternative method to estimate the transmission rate [27].

When the incident pulse is applied to the transducer A, the sound pulse is transmitted through the rod A, sample and rod B successively, and reaches the transducer B. Here the voltage generated at the transducer B in this way is denoted by V_{AB}. Since fairly long buffer rods are necessary for the measurements at high temperatures, the sound attenuation due to the quartz rods is no longer negligible. Therefore, we measured not only V_{AB} but also the voltages, V_{AA} and V_{BB}, which are generated at the transducers A and B, respectively, by the echo signals reflected from the interface between the liquid sample and the buffer rods. In addition we also measured the transmission signal V_{BA} to confirm the validity of the present method. These quantities may be expressed as follows [1]:

$$V_{AB} = V_0 \alpha_A T_A t_{AS} T_S t_{SB} T_B \beta_B \tag{3a}$$

$$V_{BA} = V_0 \alpha_B T_B t_{BS} T_S t_{SA} T_a \beta_A \tag{3b}$$

$$V_{AA} = V_0 \alpha_A T_A r_{AS} T_A \beta_A \tag{3c}$$

$$V_{BB} = V_0 \alpha_B T_B r_{BS} T_B \beta_B \tag{3d}$$

where V_0 is the voltage of the incident pulse and $T_A(T_B)$ the transmission rate through the buffer rod A (B). α_A (α_B) is the efficiency of the transducer A (B) in converting the electric voltage to the sound pressure, and β_A (β_B) is the efficiency in the inverse process. r_{AS} (r_{BS}) is the reflectivity of the sound pressure at the interface between the buffer rod A (B) and the liquid sample, and t_{AS} (t_{SB}) is the transmissivity. Both r_{AS} (r_{BS}) and t_{AS} (t_{SB}) can be calculated from the acoustic impedance [1], which is the product of the density and sound velocity [28].

Making use of equations (3*a*), (3*c*) and (3*d*), one can obtain the following formula for the transmission rate T_S(A→B) through the sample from A to B:

$$T_S(\mathrm{A} \rightarrow \mathrm{B}) = \frac{V_{AB}}{\sqrt{V_{AA} V_{BB}}} \frac{\sqrt{|r_{AS}||r_{BS}|}}{|t_{AS}||t_{SB}|} \sqrt{\frac{\alpha_B \beta_A}{\alpha_A \beta_B}}. \tag{4a}$$

Similarly from equations (3*b*), (3*c*) and (3*d*) the transmission rate from B to A, T_S(B→A), is expressed as

$$T_S(\mathrm{B} \rightarrow \mathrm{A}) = \frac{V_{BA}}{\sqrt{V_{AA} V_{BB}}} \frac{\sqrt{|r_{AS}||r_{BS}|}}{|t_{BS}||t_{SA}|} \sqrt{\frac{\alpha_A \beta_B}{\alpha_B \beta_A}}. \tag{4b}$$

The last term of equation (4*a*), $\sqrt{\alpha_B \beta_B / \alpha_A \beta_B}$, was determined by equating

$$T_S(\mathrm{A} \rightarrow \mathrm{B}) = T_S(\mathrm{B} \rightarrow \mathrm{A}) \tag{5}$$

and it proved to be nearly constant (within 4%) throughout the measurements.

The relative error in the attenuation coefficient, $|\Delta\alpha/\alpha|$, is expressed from equation (2), as follows [1],

$$\left| \frac{\Delta\alpha}{\alpha} \right| \leqslant \left| \frac{\Delta T_S}{T_S \ln T_S} \right| + \left| \frac{\Delta l_S}{l_S} \right|. \tag{6}$$

Here ΔT_S is the error of the transmission rate and Δl_S is the error of the sample thickness. It is evident from the inequality (6) that the error limit of α becomes large not only when T_S approaches null but also when it approaches unity. Thus the data are considered to be reliable when the T_S value lies between 0.05 and 0.7, and for this purpose we selected an optimal sample thickness for each frequency. The upper limit of the relative error of α was evaluated to be 20% throughout the present work.

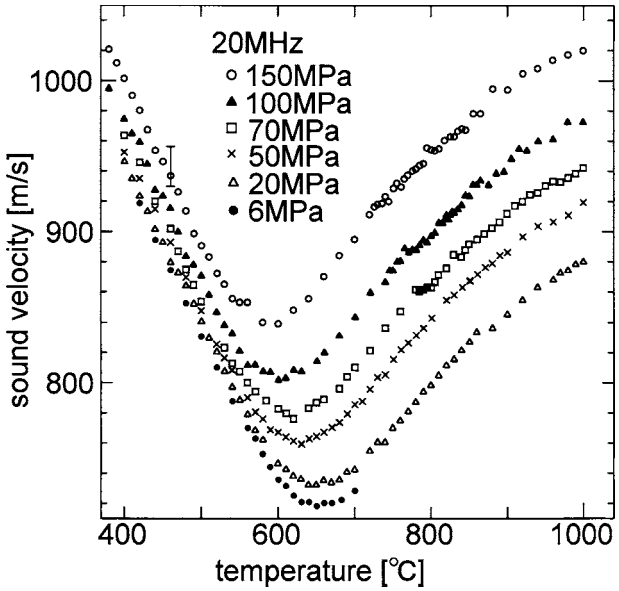

Figure 3. The sound velocity at 20 MHz is shown as a function of temperature. Several different symbols are used depending on the pressure. A typical error bar is shown in the figure.

3. Results

3.1. Sound velocity

Figure 3 shows the temperature dependence of v measured at 20 MHz along the experimental paths shown in figure 1. Near the melting point v decreases with increasing temperature and it begins to increase at higher temperatures. This behaviour was first found by Yao *et al* [18] and confirmed by subsequent works [19, 20]. The temperature, T_{min}, where v exhibits the minimum, is about 650 °C at 6 MPa in the present work, which is higher than the value reported by Yao *et al* [18], and slightly lower than those by Takimoto and Endo [19] and Tsuchiya [20] at atmospheric pressure. Such discrepancy may be due to ambiguities in the temperature calibration in the previous measurements. As the pressure increases, v increases rapidly and T_{min} shifts to lower temperatures. The overall feature is very similar to the work by Takimoto and Endo [19].

The sound velocity was also measured at 32 and 43 MHz but no appreciable dispersion was observed.

3.2. Sound attenuation

The sound attenuation coefficient divided by the square of frequency, α/f^2, is shown for 20, 32 and 43 MHz as a function of temperature in figures 4(a), (b) and (c), respectively. Here the data taken at 50, 100 and 150 MPa are selected. We measured α both on heating and cooling runs, and confirmed the reproducibility of the data. As shown in the figures, α depends strongly on temperature, pressure and frequency.

For 20 MHz, α/f^2 at 50 MPa decreases rapidly near the melting point to a small value, and begins to increase near 750 °C, exhibiting a maximum around 850 °C. The maximum around 850 °C becomes more prominent at higher pressures. In addition a hump grows near

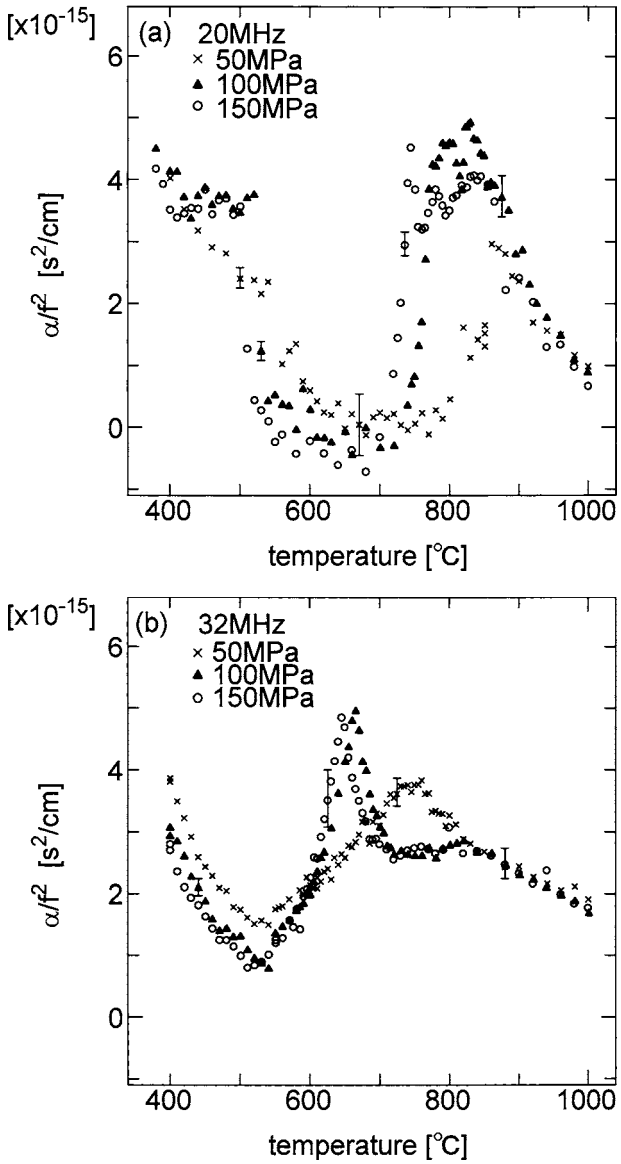

Figure 4. The attenuation coefficient divided by the square of frequency, α/f^2, at 20 MHz (a), at 32 MHz (b) and at 43 MHz (c) is shown as a function of temperature. The data taken at 50, 100 and 150 MPa are selected. Three different symbols are used depending on the pressure. Typical experimental uncertainties are indicated by the error bars.

500 °C with increasing pressure. For 32 MHz, α/f^2 shows a minimum instead of a hump near 500 °C, and a broad peak is seen around 750 °C at 50 MPa. With increasing pressure, the peak at 750 °C becomes separated into two peaks: a sharp peak around 650 °C and a diffuse one around 850 °C. For 43 MHz, the temperature variation of α/f^2 at 50 MPa is structureless except for small humps around 500 and 750 °C. However, the hump around 750 °C becomes larger with increasing pressure, and at 150 MPa it seems to consist of two overlapping peaks around 700 and 850 °C.

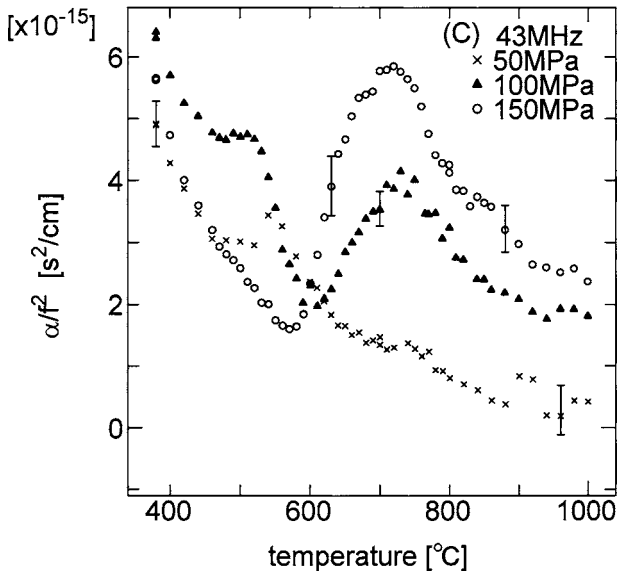

Figure 4. (Continued)

4. Analysis

To analyse the observed complicated behaviour of α, we begin with a standard formula for the sound attenuation in liquids [29]:

$$\frac{\alpha}{f^2} = \frac{2\pi^2}{\rho v^3}\left\{\left(\zeta + \tfrac{4}{3}\eta\right) + \kappa\left(\frac{1}{C_v} - \frac{1}{C_p}\right)\right\} \tag{7}$$

where f is the frequency, ζ and η are the bulk viscosity and shear viscosity, respectively, κ is the thermal conductivity and C_v and C_p are the specific heats at constant volume and pressure, respectively. Perron [25] measured the thermal conductivity of Se_xTe_{1-x} mixtures for $x \leqslant 0.4$ at atmospheric pressure and obtained a relation:

$$\kappa = \kappa_R + L\sigma T \tag{8}$$

with the residual thermal conductivity $\kappa_R = 3.5$ mW cm^{-1} °C^{-1}, the Lorenz number $L = 2 \times 10^{-8}$ V^2 °C^{-2} and σ the electrical conductivity. We have estimated the thermal conductivity term, $(2\pi^2/\rho v^3)\kappa(1/C_v - 1/C_p)$, by using equation (8) and available data for σ [14], C_p [21] and density [15], which reveals that this term is less than 1% of the observed α/f^2. Hence, equation (7) may be rewritten as

$$\zeta + \tfrac{4}{3}\eta \simeq \frac{\alpha\rho v^3}{2\pi^2 f^2} \equiv \alpha^*. \tag{9}$$

In figure 5 α^* as defined above are plotted for 32 MHz at various pressures as a function of the reciprocal temperature in the temperature range below 500 °C. The figure also includes the temperature dependence of η for liquid $Te_{50}Se_{50}$, which is estimated as a arithmetic mean of η between $Te_{40}Se_{60}$ and $Te_{60}Se_{40}$ at atmospheric pressure [24]. It is evident that in the low temperature range α^* varies almost linearly with $1/T$ with nearly the same slope as η and that α^* is larger than η by a factor of 2 to 3, suggesting that the ratio ζ to η is nearly unity as is often the case of viscoelastic liquids [30]. This is a reasonable result, because near the

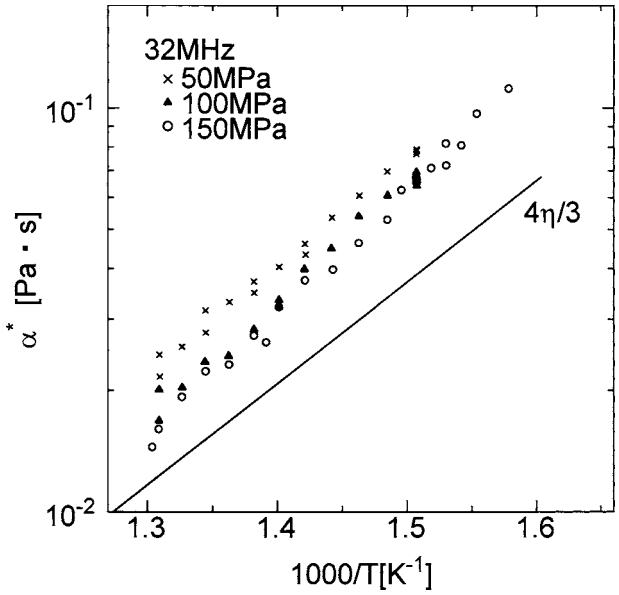

Figure 5. α^* defined by equation (9) is plotted against the reciprocal temperature. Here the data below 500 °C at 32 MHz are shown, together with temperature dependence of the shear viscosity η for $Se_{50}Te_{50}$ estimated from [24]. Three different symbols are used depending on the pressure.

melting point liquid $Te_{50}Se_{50}$ has an Se-like structure composed of chain molecules and the chain length becomes shorter with increasing temperature.

Next we assume that the bulk viscosity ζ can be divided into a normal term ζ_N, which obeys the same Arrhenius law as η, and an anomalous term ζ_A:

$$\zeta = \zeta_N + \zeta_A \tag{10}$$

$$\zeta_N + (4/3)\eta = A(P)\exp[B(P)/k_BT] \tag{11}$$

where $A(P)$ and $B(P)$ are independent of temperature but depend on pressure. Then the anomalous term may be given by

$$\zeta_A = \alpha^* - A(P)\exp[B(P)/k_BT]. \tag{12}$$

By treating $A(P)$ and $B(P)$ as fitting parameters, we have fitted equation (11) to the observed α^* for 32 MHz in the temperature range below 500 °C, and by using the resultant $A(P)$ and $B(P)$ parameters we have extracted the anomalous term ζ_A in the whole temperature range of the present experiment. As seen in figure 6, ζ_A is almost flat up to 500 °C, where it begins to rise rapidly. At 150 MPa there exists a narrow peak at 630 °C and a broad peak around 850 °C, while at 50 MPa there is apparently one broad peak. Our naïve picture is that at high pressures, where a chain molecule exists very close to the adjacent one, the application of pressure should have some definite influences upon the inter-chain correlation, while at low pressures, where there is more free space among chain molecules, such influences could be blurred. From this point of view we try to resolve the peak at 50 MPa into two sub-peaks. In figure 6, the solid lines denote these sub-peaks expressed by Gaussian functions and the dash–dotted line denotes their sum. The dash–dotted line in figure 6 reproduces the original peak well.

In contrast to the data for 32 MHz, a hump already exists below 500 °C in the temperature variation of α for 20 MHz, which prevents us from fitting equation (11) to the data directly. Thus we have tentatively utilized the same parameters $A(P)$ and $B(P)$ as those for 32 MHz,

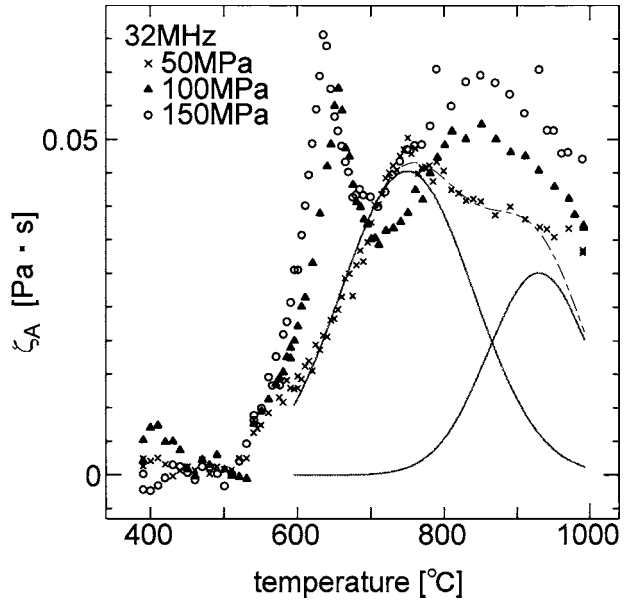

Figure 6. The anomalous term of the bulk viscosity, ζ_A, at 32 MHz is shown as a function of temperature. The solid lines denote the two components resolved from the peak at 50 MPa and the dash–dotted line denotes the sum of these components. Three different symbols are used depending on the pressure.

and deduced by ζ_A using equation (12). Then, as shown in figure 7, we find that peaks, which grow up with pressure, are seen around 450 and 850 °C and ζ_A remains nearly zero at intermediate temperatures, where the sharp peak was observed for 32 MHz.

For 43 MHz, we have adopted two methods to subtract the term $A(P)\exp[B(P)/k_BT]$. One is a direct fitting to the low temperature data, and the other is to use the same parameters $A(P)$ and $B(P)$ as those for 32 MHz. The resulting ζ_A by the former method is shown in figure 8(a) and the latter in figure 8(b). Although the behaviours below 600 °C are very different from each other, the shapes of ζ_A at high temperatures are nearly identical. This is not surprising because the normal term is substantially reduced at high temperatures. We have tentatively separated the high temperature peak into two sub-peaks by using Gaussian functions, as shown by the solid lines.

Based upon these observations, we may summarize the characteristic features of the present results, as follows. First, there exist two peaks in the temperature variation of α. One is the high temperature peak, which appears around 850 °C irrespective of the frequency, and the other is the low temperature peak, whose position depends strongly on the frequency. Secondly, the width of the low temperature peak is relatively narrow compared with that of the high temperature peak. Thirdly, both peaks become more prominent with increasing pressure.

To illustrate these features more clearly, the positions of the high and low temperature peaks are plotted in figure 9 as a function of pressure, together with the locus of T_{min}, where the sound velocity exhibits the minimum. The peak positions change little with pressure. At 100 and 150 MPa, where the peaks are clearly seen, the positions of the low temperature peak are arranged with a nearly equal spacing in accordance with the difference in the frequency. Figures 10(a) and (b) show the height of the low and high temperature peaks, respectively, as a function of pressure. The height of the high temperature peak has a clear frequency

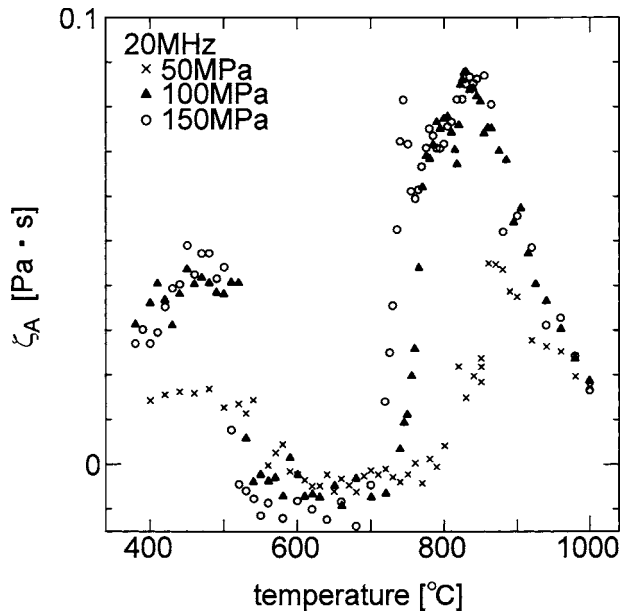

Figure 7. The anomalous term of the bulk viscosity, ζ_A, for 20 MHz deduced by utilizing the same parameters $A(P)$ and $B(P)$ as those for 32 MHz is shown as a function of temperature. Three different symbols are used depending on the pressure.

dependence. The lower the frequency is, the higher the peak is, and the height begins to rise at lower pressures for the lower frequency. The height of the low temperature peak also increases rapidly with pressure.

5. Discussion

When the volume change occurs out of phase with the applied sound pressure, the bulk viscosity becomes large. Thus it is proportional to the imaginary part of the inverse of the frequency dependent adiabatic compressibility, $\beta(\omega)$ [30],

$$\zeta = \frac{\mathrm{Im}(1/\beta(\omega))}{\omega} \tag{13}$$

where ω is the angular frequency ($=2\pi f$). In the previous paper [1] we interpreted the anomalous sound attenuation of liquid Hg in the metal–nonmetal transition range as a Debye-type relaxation in a two-level system, where we consider that the sound pressure may give rise to switching from nonmetallic to metallic and *vice versa*. Recent results of α in Hg with different frequencies [31] further support our previous discussion [1]. In the Debye model the relaxation time τ_D is related to $\beta(\omega)$, as follows [32]:

$$\beta(\omega) = \beta_\infty + \frac{\beta_0 - \beta_\infty}{1 + \mathrm{i}\omega\tau_D} \tag{14}$$

where β_0 is the static adiabatic compressibility ($\beta_0 = 1/\rho v^2$) and β_∞ is the adiabatic compressibility at frequencies beyond the radio frequency range. Then ζ is rewritten as

$$\zeta = \frac{(\beta_0 - \beta_\infty)\tau_D}{\beta_0^2 + \omega^2\tau_D^2\beta_\infty^2}. \tag{15}$$

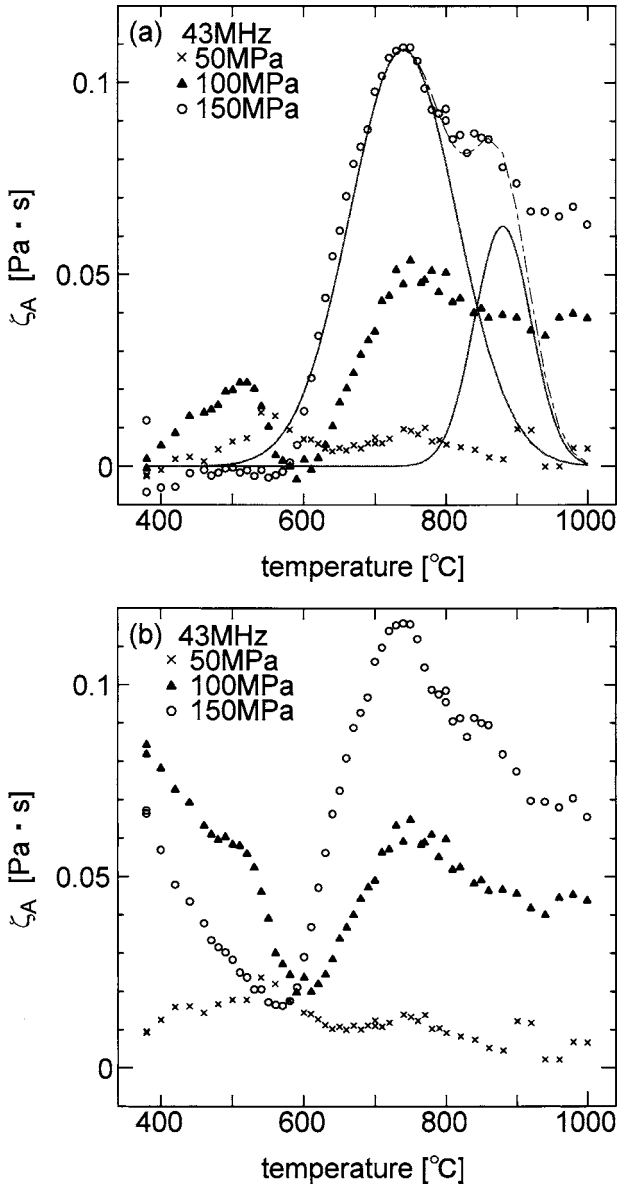

Figure 8. The anomalous term of the bulk viscosity, ζ_A, at 43 MHz is shown as a function of temperature. Three different symbols are used depending on the pressure. The subtraction of the low temperature part is done by a direct fitting (a), and by using the same parameters as those at 32 MHz (b). In (a), the solid lines denote the two components expressed by Gaussian functions and the dash–dotted line denotes the sum of these components.

As shown in figure 10(b), the height of the high temperature peak has a frequency dependence that is consistent with equation (15). Since ζ_N is negligible at 850 °C, we can put simply, $\zeta = \zeta_A$. As an example, ζ_A at 100 MPa is plotted against the frequency in figure 11. The solid line described by equation (15) with $\tau_D = 6.7$ ns and $\beta_\infty = 2.47 \times 10^{-10}$ Pa^{-1} fits the data, implying a slow dynamics. It should be noted, however, that the fraction of the relaxation part

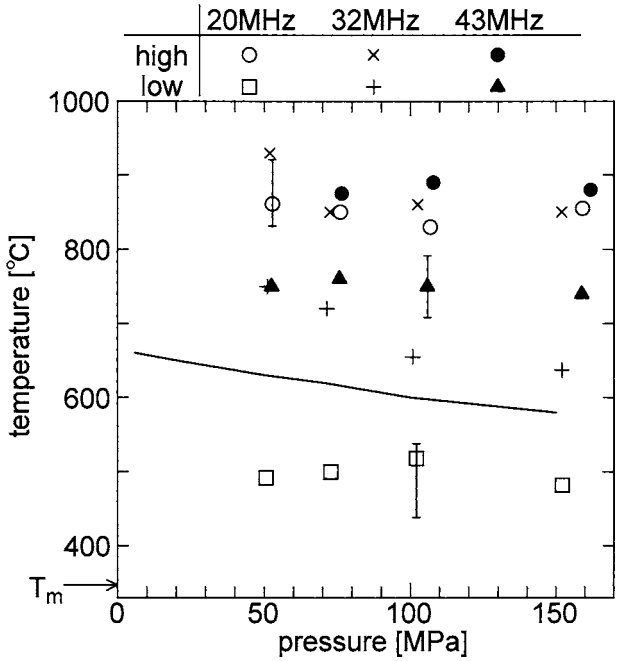

Figure 9. The peak position in the temperature variation of ζ_A is plotted as a function of pressure for various frequencies. The solid line shows the locus of T_{min}, where the sound velocity exhibits the minimum. The meaning of these symbols is tabulated above the figure. The melting point, T_m, of $Se_{50}Te_{50}$ (345 °C) is indicated by the arrow. Typical error bars are shown in the figure.

of $\beta(\omega)$, $(\beta_0 - \beta_\infty)/\beta_0$, is less than 0.5%, which is consistent with the fact that no appreciable dispersion was observed in the sound velocity. The value of τ_D for $Te_{50}Se_{50}$ is larger than that for monatomic liquid Hg (less than 4 ns) [31]. This is not unreasonable, because the average chain length in liquid $Te_{50}Se_{50}$ is estimated to be about seven atoms at 850 °C from magnetic susceptibility data [32] (see also figure 13).

By contrast the low temperature peak cannot be interpreted by the simple Debye model, because ζ_A does not monotonically decrease with frequency. Based upon the evidence that the low temperature peak moves to higher temperatures with increasing frequency, we suppose that there may be a time scale τ_{ch} which characterizes the inter-chain rearrangements and which varies with temperature. In polymer physics the sound attenuation is often discussed in connection with changes in the intra-chain conformation (e.g. *trans*-to-*gauche* conversion) [33], which should be hindered by adjacent chains under high pressure. For liquid $Te_{50}Se_{50}$ such behaviour is expected to be observed near the melting point. In fact, the normal term expressed by equation (11) decreases with increasing pressure, as shown in figure 5. Since the height of the low temperature peak *increases* with pressure, the peak must be associated with the inter-chain rearrangements. At the temperature of the peak position we have simply taken the inverse of the relevant frequency as τ_{ch}. In figure 12 τ_{ch} estimated from the data at 100 MPa is plotted as a function of temperature together with τ_D. A smooth extrapolation of τ_{ch} would give a value around 16 ns at 850 °C, which is comparable with τ_D. In figure 13 these relaxation times are plotted against the average number of atoms per chain estimated from the magnetic susceptibility [32].

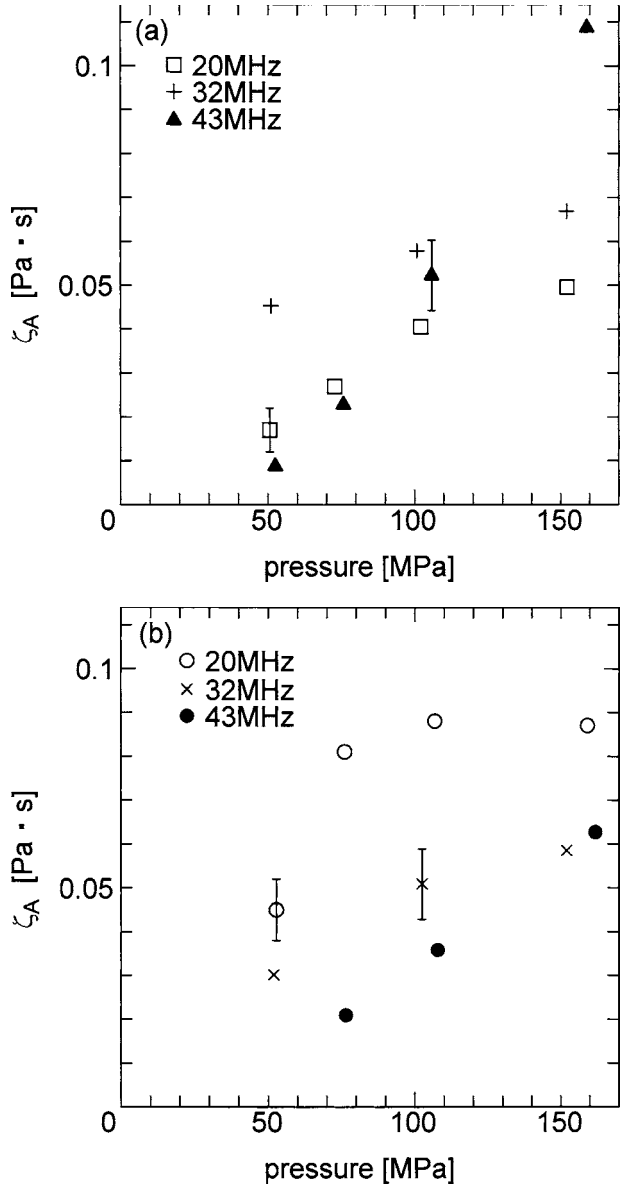

Figure 10. The height of low temperature peaks (a) and high temperature peaks (b) are plotted against the pressure. The meaning of these symbols is according to figure 9. Typical error bars are shown in the figure.

Recently the time evolution of local chain structure has been discussed in liquid Se by means of *ab initio* molecular-dynamics simulations [34–36], which demonstrate that bond breaking and re-arrangement of chains take place in a sub-picosecond time scale [36]. To explain the anomalous sound attenuation in liquid $Te_{50}Se_{50}$, however, the more cooperative nature of the inter-chain re-arrangements should be taken into account, because the time scale in the present study is larger by more than three orders of magnitude. As to the anomalous sound attenuation in the metal–nonmetal transition range of liquid Hg, we made a speculation

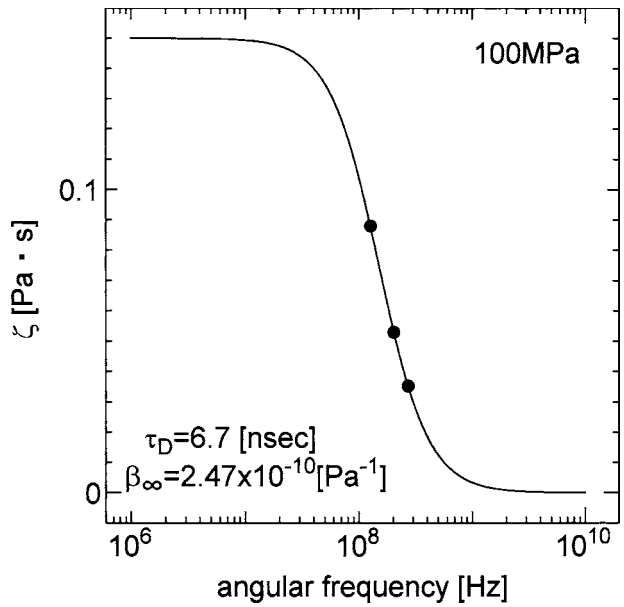

Figure 11. The peak value of the high temperature part of ζ_A at 100 MPa is plotted against the frequency. The solid line is described by equation (15) with $\tau_D = 6.7$ ns and $\beta_\infty = 2.47 \times 10^{-10}$ Pa^{-1}.

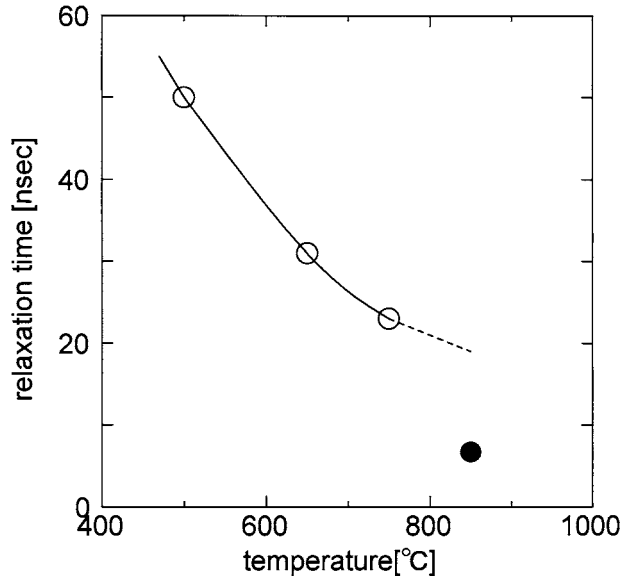

Figure 12. τ_{ch} estimated from the data at 100 MPa is plotted by the open circles as a function of temperature. τ_D is also plotted by an closed circle. The line in the figure is a guide for the eyes.

that, when a local region could be switched from nonmetallic to metallic by the sound pressure, it would be stabilized due to the metallic cohesion and remain metallic for a short time even after the sound pressure is removed [1]. It has been suggested for liquid Te [11–13] that, although twofold coordinated chain structure is preserved even in the metallic state, the chains

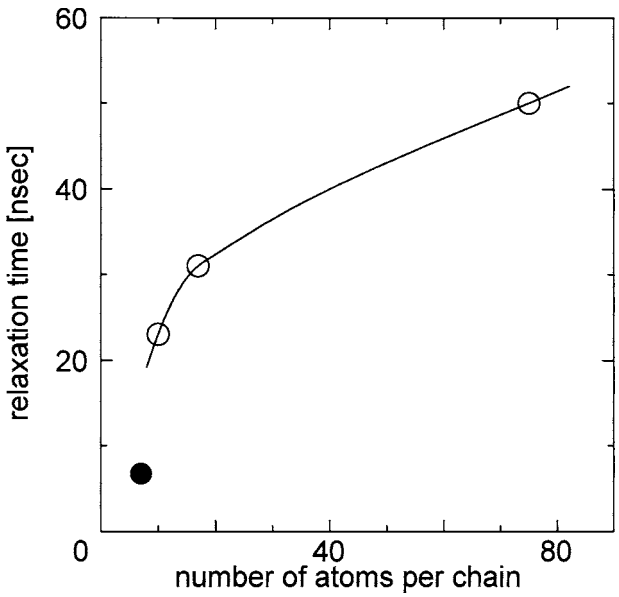

Figure 13. τ_{ch} is plotted by the open circles against the average number of atoms per chain estimated from the magnetic susceptibility [32]. τ_D is also plotted by a closed circle. The thin line is a guide for the eyes.

are no longer helical but some of the covalent bonds are elongated by inter-chain charge transfer. This picture has been successfully applied to liquid Te–Se mixtures [37] and liquid Se under pressure [38]. Inferring from a high pressure crystalline form of Te, in which planar zigzag chains with long and short covalent bonds are stacked in the direction perpendicular to the plane [39], one could expect a zigzag-like local structure in liquid Te and also in Te–Se mixtures. Once such a zigzag-like structure was formed, it could be stabilized by the metallic cohesion.

It may be instructive to refer to our recent studies [40, 41] on the dielectric relaxation of supercritical water to think about a possible relation between sub-picosecond phenomena and nanosecond relaxation. Unexpectedly the relaxation time increases rapidly with decreasing density in the gaseous state, indicating that an isolated water molecule would have a very long relaxation time [41]. We have explained this phenomenon by considering that the applied electric field can hardly change the thermal motion of water molecule as long as it is rotating, and that only when it loses angular momentum by colliding with another molecule, can the electric field control the molecule orientation. This means that the molecule is sensitive to the applied field only on special occasions. Extending this idea to the acoustic response of liquid Te–Se mixtures, one could expect that the chain molecules become sensitive to the sound pressure when they happen to have a zigzag-like structure after many stochastic processes of bond breaking and re-connecting. At low temperatures such structural modification would take more time because the chains are longer and more stabilized.

6. Summary and outlook

The sound attenuation coefficient α of liquid $Te_{50}Se_{50}$ has been measured at 20, 32 and 43 MHz in the temperature and pressure range up to 1000 °C and 150 MPa. Near the melting point α

decreases with increasing temperature, which is explained by the temperature variation of shear viscosity [23]. In addition to the normal behaviour, we have found two peaks in the temperature variation of α. One is the high temperature peak, which appears around 850 °C irrespective of the frequency, and the other is the low temperature peak, whose position depends strongly on the frequency. Both peaks become more prominent with increasing pressure, indicating the importance of the inter-chain couplings. Assuming a Debye-type relaxation for the frequency-dependent adiabatic compressibility, we have estimated the relaxation time to be about 7 ns from the high temperature peak.

We are now extending the acoustic measurements to other systems in which the metal–nonmetal transition is observed, to investigate whether the slow dynamics in the metal–nonmetal transition range is a universal phenomenon like that at the liquid–gas critical point [42] and liquid–glass transition [43].

Acknowledgments

The authors are grateful to Mr K Furuta for collaboration on the experiments. We also thank Professors H Endo and F Hensel for valuable discussions. This work was partially supported by a Grant-in-Aid for Scientific Research from the Ministry of Education, Science, Sports and Culture, Japan. The manuscript was written during the stay of MY in Marburg, Germany, which was financially supported by the Alexander von Humboldt Foundation.

References

[1] Kohno H and Yao M 1999 *J. Phys.: Condens. Matter* **11** 5399
[2] Kohno H, Okada K, Kajihara Y, Hiejima Y and Yao M 1999 *J. Non-Cryst. Solids* **250–252** 139
[3] Kozhevnikov V F, Arnold D I, Briggs M E, Naurzakov S P, Viner J M and Taylor P C 1999 *J. Acoust. Soc. Am.* **106** 3424
[4] Perron J P 1967 *Adv. Phys.* **16** 657
[5] Misawa M and Suzuki K 1977 *Trans. Japan Inst. Met.* **18** 427
[6] Eisenberg A and Tobolsky A V 1960 *J. Polym. Sci.* **46** 19
[7] Warren W W Jr and Dupree R 1980 *Phys. Rev.* B **22** 2257
[8] Tourand G and Breuil 1971 *J. Physique* **32** 813
[9] Cabane B and Friedel J 1971 *J. Physique* **32** 73
[10] Enderby J E and Barnes A C 1990 *Rep. Prog. Phys.* **53** 85
[11] Endo H 1993 *J. Non-Cryst. Solids* **156–158** 667
[12] Tsuzuki T, Yao M and Endo H 1995 *J. Phys. Soc. Japan* **64** 485
[13] Kawakita Y, Yao M and Endo H 1999 *J. Non-Cryst. Solids* **250–252** 695
[14] Yao M, Misonou M, Tamura K, Ishida K, Tsuji K and Endo H 1980 *J. Phys. Soc. Japan* **48** 109
[15] Thurn H and Ruska J 1976 *J. Non-Cryst. Solids* **22** 331
[16] Menelle A, Bellissent R and Flank A M 1989 *Physica* B **156/157** 174
[17] Hoyer W, Neumann and Wobst N 1992 *Z. Naturf.* **479** 833
[18] Yao M, Suzuki K and Endo H 1980 *Solid State Commun.* **34** 187
[19] Takimoto K and Endo H 1982 *Phys. Chem. Liq.* **12** 141
[20] Tsuchiya Y 1991 *J. Phys. Soc. Japan* **60** 960
[21] Takeda S, Okazaki H and Tamaki S 1985 *J. Phys. Soc. Japan* **54** 1890
[22] Tsuchiya Y 1988 *J. Phys. Soc. Japan* **57** 3851
[23] Kakinuma F and Suzuki K 1993 *Z. Metallkd.* **84** 541
[24] Perron J C, Rabit J and Rialland J F 1982 *Phil. Mag.* B **46** 321
[25] Perron J C 1970 *Phys. Lett.* A **32** 169
[26] Suzuki K, Inutaki M, Fujiwaka S, Yao M and Endo H 1980 *J. Physique Coll.* **4** C8 66
[27] Yao M, Okada K, Aoki T and Endo H 1996 *J. Non-Cryst. Solids* **205–207** 274
[28] Truell R, Elbaum C and Chick B B 1969 *Ultrasonic Methods in Solid State Physics* (New York: Academic) ch 2
[29] Hansen J-P and McDonald I R 1986 *Theory of Simple Liquids* 2nd edn (London: Academic) ch 8
[30] Litovitz T A and Davis C M 1965 *Physical Acoustics* vol II, ed W P Mason (New York: Academic) ch 5

[31] Kohno H and Yao M in preparation
[32] Misonou M and Endo H 1982 *Ber. Bunsenges. Phys. Chem.* **86** 645
[33] Lamb J 1965 *Physical Acoustics* vol II, ed W P Mason (New York: Academic) ch 4
[34] Hohl D and Jones R O 1991 *Phys. Rev.* B **43** 3856
[35] Kirchhoff F, Kresse G and Gillan M J 1998 *Phys. Rev.* B **57** 10 482
[36] Shimojo F, Hoshino K, Watabe M and Zempo Y 1998 *J. Phys.: Condens. Matter* **10** 1199
[37] Tamura K, Inui M, Yao M, Endo H, Hosokawa S, Hoshino H, Katayama Y and Mruyama K 1991 *J. Phys.: Condens. Matter* **3** 7495
[38] Tsuji K, Shimomura O, Tamura K and Endo H 1988 *Z. Phys. Chem., N.F.* **156** 495
[39] Aoki K, Shimomura O and Minomura S 1980 *J. Phys. Soc. Japan* **48** 551
[40] Okada K, Imashuku Y and Yao M 1997 *J. Chem. Phys.* **107** 9302
[41] Okada K, Yao M, Hiejima Y, Kohno H and Kajihara Y 1999 *J. Chem. Phys.* **110** 3026
[42] Kawasaki K 1976 *Phase Transitions and Critical Phenomena* vol 5a, ed C Domb and M S Green (London: Academic) ch 4
[43] Hopkins L and Kurkjian C R 1965 *Physical Acoustics* vol II, ed W P Mason (New York: Academic) ch 8